



## Kinetics and Mechanism of the Adsorption of Methylene Blue from Aqueous Solution onto Turkish Green Clay

Özkan Demirbaş<sup>1\*</sup> and Mehmet Salih Nas<sup>2</sup>

<sup>1</sup>Department of Chemistry, Faculty of Science and Literature, University of Balıkesir, Balıkesir, Turkey.

<sup>2</sup>Department of Chemistry, Faculty of Science and Literature, University of Yüzüncü Yıl, Van, Turkey.

### Authors' contributions

This work was carried out in collaboration between both authors. Author OD designed the study, wrote the protocol and the first draft of the manuscript. Author MSN performed the lab experiments, statistical analysis and managed the literature search. Both authors read and approved the final manuscript.

### Article Information

DOI: 10.9734/ACRI/2016/30677

#### Editor(s):

(1) Sivakumar Manickam, Department of Chemical and Environmental Engineering, The University of Nottingham Malaysia Campus, Malaysia.

#### Reviewers:

(1) Atiya Firdous, Jinnah University for Women, Pakistan.

(2) Muhammad Raziq Rahimi Kooh, University of Brunei Darussalam, Brunei.

(3) M. Mupa, Bindura University of Science Education, Zimbabwe.

Complete Peer review History: <http://www.sciencedomain.org/review-history/17313>

Original Research Article

Received 24<sup>th</sup> November 2016

Accepted 18<sup>th</sup> December 2016

Published 22<sup>nd</sup> December 2016

### ABSTRACT

In this study, the thermodynamic parameters and adsorption kinetics of methylene blue (MB) onto Turkish green clay (TGC) from Gurpinar in Van, Turkey were investigated in aqueous solution through batch adsorption experiment. Turkish green clay was used in this study for the first time in the literature for this purpose. Adsorption studies were carried out to investigate the effect of experimental factors such as contact time (1-120 min), initial dye concentration ( $0.5-2.0 \times 10^{-5}$  M), temperature (298-328 K) and pH (5.5-9) on the adsorption of MB. The Turkish green clay (TGC), methylene blue (MB) and MB adsorbed Turkish green clay (MB-TGC) were characterized by SEM, FTIR-ATR, TGA and BET surface area analysis. Three different kinetic models, pseudo-first-order, pseudo-second-order and intraparticle diffusion were used to fit the kinetics data. The pseudo-second-order model best described the experimental data. However, the adsorption of MB was more suitable to be controlled by an intra-particle diffusion mechanism. The thermodynamic activation parameters, such as enthalpy, entropy and Gibbs free energy were determined. The

\*Corresponding author: Email: [ozkandemirbas@gmail.com](mailto:ozkandemirbas@gmail.com);

maximum adsorption capacity of TGC was found to be 195.74 mg/g (or 0.612 mmol/g) at pH 9, 298 K and  $2.0 \times 10^{-5}$  M, initial MB concentration of solution. These results showed that MB can be effectively removed from aqueous solution employing TGC as an adsorbent.

*Keywords: Thermodynamics; adsorption; methylene blue; Turkish green clay; kinetics; characterization.*

## 1. INTRODUCTION

Water containing dyes is one of the most hazardous chemical compound classes found in the industrial waste water [1]. This waste can seriously cause medical effects such as allergy, dermatitis, skin irritation, cancer, mutation, etc. [1-3]. For this reason, it is very important to remove the dyestuffs from the waste water to protect the unpolluted natural water [4]. Frequently used in the textile industry, methylene blue (MB) is a heterocyclic aromatic compound having the chemical formula  $C_{16}H_{18}N_3S$ . Wastewaters containing dyes, such as methylene blue, contain toxic substances which are harmful to animals and plants [5]. For this reason, one of the major problems concerning textile wastewaters is the treatment of colored effluent.

In recent years, various processing technologies have been developed to decolorize dyeing wastewater. These processes include biological [6], physio-chemical [7], membrane filtration [8], ozonation [9] and advanced oxidation [10] and integrated treatment processes [11]. However, these processes are costly for large systems [12]. The adsorption method used in this study is one of the simplest, fastest and most cost-effective techniques that can be used as an alternative to these processes to remove harmful organic synthetic dyes from aqueous solutions and industrial waste water [13]. The efficiency of the adsorption process is highly dependent on the characteristics of the adsorbent used in the process [14,15]. The most preferred type of adsorbent for adsorption processes is active carbon with high surface area and adsorption capacity [15-17]. Despite the high adsorption capacity, commercial activated carbon is one of the more expensive adsorbents. Alternatively, clay based adsorbents are used as promising adsorbents in the treatment of wastewater in many studies [18,19]. The clays have certain properties that make them an ultimate choice for adsorption, such as low cost, high availability and environmentally friendly materials [20]. Many adsorbents for adsorption of methylene blue from aqueous solution have been extensively studied

in the literature. Some of them are magnetic graphene-carbon nanotube composite [21], garlic peel [22], CEN [23], and breadnut core [24] etc.

The green clay used in the study is really green. Green clay, also known as French green clay in the literature, is an organic material comprised of a host of essential minerals, iron oxides, and decomposed plant material such as kelp and seaweed. Illite was called French green clay for centuries, named after the rock quarries in the south of France that yielded most of the world's illite deposits. Green clays are used in alternative medicine, both externally and internally, for many reasons, but mostly for cleaning and detox because of its vast absorbent properties. In recent years, Williams et al. [25, 26] has reported that green clay heals Buruli ulcers. They assessed the antibacterial properties of this clay and said it could provide a cheap treatment for other skin infections. However, the green clay used in the study was obtained from the mineral deposits in the Gürpınar district of Van in Turkey. Therefore, the name is called Turkish green clay.

The aim of this study was to determine the adsorption kinetics of MB onto Turkish green clay (TGC) over a range of physicochemical conditions, which is important to identify various natural environmental systems. Samples of TGC, MB and MB adsorbed Turkish green clay (MB-TGC) were characterized by SEM, FTIR-ATR, TGA and BET apparatus. A number of experimental parameters in this study are considered, including the effect of contact time, initial MB concentration, pH and temperatures. Adsorption of MB dye was tested in batch and their kinetic parameters were determined. The thermodynamic activation parameters of the process, such as entropy, enthalpy and the Gibbs free energy, also determined.

## 2. MATERIALS AND METHODS

### 2.1 Materials

The raw TGC used in this work were collected from Gurpınar regions in Van, Turkey and some

analyses were performed for its characterization. The specific surface area of TGC was measured by BET N<sub>2</sub> adsorption by Micromeritics FlowSorb II-2300 equipment. The BET surface and pore volumes were calculated from the N<sub>2</sub> adsorption isotherms. The morphologies of samples were observed in scanning electron microscopy (SEM) of JEOL, Japan. Fourier transform infrared (FTIR) spectra were recorded on a PerkinElmer FTIR spectrometer using ATR device. The Thermo-Gravimetric (TG) analysis was obtained simultaneously using a Perkin Elmer instrument. All the chemicals were of analytical grade and were used without any further purification. Methylene blue hydrate was purchased from Sigma-Aldrich. The concentration of MB dye was measured at  $\lambda_{\max} = 662$  nm using Perkin Elmer UV-Visible spectrophotometer.

## 2.2 Experimental Procedure

Adsorption kinetic experiments were carried out using mechanic stirrer. All of the MB solution was prepared with ultra pure water. Kinetic experiments were carried out by agitating 1000 mL of MB solution of initial concentration  $1.0 \times 10^{-5}$  M at a constant agitation speed of 600 rpm, 298 K and pH 9. Agitation was done for 120 min, which is more sufficient than time to reach equilibrium at a constant agitation speed of 600 rpm. Preliminary experiments had shown the effect of the separation time on the adsorbed amount of MB. The initial tested concentration of MB solution was 0.5, 1.0 and  $2.0 \times 10^{-5}$  M. The effect of pH on TGC of MB was analysed in the pH range from 5.5 to 9. The pH was adjusted using 0.05 N NaOH and 0.05 N HCl solutions by using an Orion 920A pH-meter with a combined pH electrode. The effect of temperature was carried out at 298, 308, 318 and 328 K in a constant temperature bath. Samples of four milliliter were drawn at suitable time intervals. The samples were then centrifuged for 5 min. at 3.000 rpm and the left out concentration in the supernatant solution was analysed using UV-Vis spectrophotometer by monitoring the absorbance changes at a wave length of maximum absorbance. Each experimental run continued until no significant change in the MB concentration was measured. The adsorbed amount of MB at any time  $t$ ,  $q_t$ , was calculated from the mass balance (Eq. (1)) [27].

$$q_t = \frac{(C_0 - C_t)}{m} \times V \quad (1)$$

where  $C_0$  and  $C_t$  (mol L<sup>-1</sup>) are the initial and liquid-phase concentrations of MB solution at any

time  $t$  (min), respectively;  $q_t$  (mmol g<sup>-1</sup>) is the amount of MB adsorbed per unit mass of TGC at time  $t$  (min),  $V$  is the volume of the adsorption (L), and  $m$  is the mass of the TGC in the solution (g).

## 3. RESULTS AND DISCUSSION

Some experimental parameters were performed in this study, including the effect of pH, contact time, initial MB concentration and temperatures. In addition, the kinetic and thermodynamic parameters of adsorption of methylene blue onto TGC surface were determined. The compound analysis (wt %) of TGC used in this work is: SiO<sub>2</sub>:44.79, MgO:20.74, Fe<sub>2</sub>O<sub>3</sub>:12.48, CaO:10.02, Al<sub>2</sub>O<sub>3</sub>:9.20, K<sub>2</sub>O:0.64, SO<sub>3</sub>:0.41, TiO<sub>2</sub>:0.49, Cr<sub>2</sub>O<sub>3</sub>:0.32, and NiO:0.26. The specific surface area and pore volume of TGC calculated as 167.2 m<sup>2</sup>g<sup>-1</sup> and 0.41 cm<sup>3</sup>g<sup>-1</sup>, respectively.

### 3.1 Effect of Solution pH

Generally, the adsorbent surfaces have ionic groups with positive and negative charges. The ions on this surface are very influenced by the pH value of the environment [28,29]. The ions on this surface are very influenced by the pH value of the environment. The net charge on the adsorbent surface is sometimes zero, depending on the pH value. Here, the pH value of the adsorbent is shown as pH<sub>pzc</sub>, where the net surface charge is zero (neutral) [23,24]. Fig. 1a shows the effect of varying the initial dye pH from 5.5 to 9 for MB in aqueous solutions when the initial concentration of dyes, temperature, and TGC dosage were kept constant. It can be seen that the amount of dye adsorbed (mmol) per unit mass of adsorbent (g) increased as pH was increased from 5.5 to 9. This can be explained by the electrostatic attraction between the positively charged MB (solution pH > pKa, MB) and the negatively charged surface of clay (solution pH > pH<sub>pzc</sub>) [23,24]. At the same time, the charge neutralization occurs at the surface of TGC which leads to the increased adsorption of MB dye molecules at elevated pH.

### 3.2 Effect of Temperature

The amounts of MB adsorbed on the TGC as function of solution temperature are shown in Fig. 1b. Fig. 1b shows the adsorption kinetics of MB at 298, 308, 318 and 328 K by plotting its uptake capacity,  $q_t$ , vs. time at the initial MB concentration of  $1.0 \times 10^{-5}$  M at pH 9. The figure indicates that the increase in solution

temperature increases the adsorbed quantities of MB. Temperature presents a notable effect on the adsorption process because it affects the diffusion of dye molecules at dye-external boundary layer interface, and also inside the adsorbent pores [27-29]. The maximum adsorption capacity ( $0.512 \text{ mmol g}^{-1}$ ) was found at 328 K. The results show that adsorption is an endothermic process.

### 3.3 Effect of Contact and Equilibrium Times and Initial MB Concentration

The adsorption of MB onto TGC at different initial concentrations (this figure not shown) and stirring speed of 600 rpm was studied as a function of contact time in order to determine the equilibrium time. Measuring the concentration of MB in solution at different incubation times generated in a time course of the adsorption. From the Table 1, it was observed that the amount of MB adsorbed gets increased from 0.208 to 0.612  $\text{mmol g}^{-1}$  for an increase in initial MB concentration from  $0.5 \times 10^{-5} \text{ M}$  to  $2.0 \times 10^{-5} \text{ M}$ . According to the Fig. 1a and b, the time required to reach a stationary concentration is about 45 min.

### 3.4 FTIR, SEM Images and Thermal Gravimetric (TG) Analyses

From the derived FTIR spectra of representative samples (Fig. 2a<sub>1</sub>, b<sub>1</sub> and c<sub>1</sub>), we inferred the following results:

- As seen in Fig. 2(a<sub>1</sub>), spectrum of TGC, the band at  $\sim 3398, 1635$  and  $1425 \text{ cm}^{-1}$  is due to H-O-H bending vibrations of adsorbed water in sheet silicate minerals. The  $\sim 950$  and  $643 \text{ cm}^{-1}$  bands arise from the Si-O-Si and Si-O vibrations.
- From Fig. 2(b<sub>1</sub>), FTIR spectrum result of MB showed peaks at  $\nu = 1593, 1488,$  and  $1389 \text{ cm}^{-1}$  mainly associated with C=C and C-N stretching vibration and C-N, anthracene band stretching vibration, respectively. The  $\sim 1334, 1249,$  and  $1139 \text{ cm}^{-1}$  bands occurs because of the vibrations of C-H,  $\text{CH}_3,$  and C-H (Ar) groups. The peaks at  $876$  and  $613 \text{ cm}^{-1}$  belonged to the C-H plane and out of plane bending vibration.
- As shown in Fig. 2(c<sub>1</sub>), FTIR spectrum obtained for MB adsorbed on TGC show the peaks of the C=C and C-N stretching vibration bands at about  $1600, 1488$  and  $1391 \text{ cm}^{-1}$ , which are typical of MB dye. As a result, the presence of characteristic peaks of MB in the spectrum indicate that the clays interact with the dye.

As can be seen clearly in Fig. 2a, b and c, the surface of TGC, MB and MB adsorbed TGC show morphological changes. According to the figures, surface morphology of the MB adsorbed TGC changed completely after 120 min. It can be concluded that the images are consistent with experimental data and FTIR spectra.

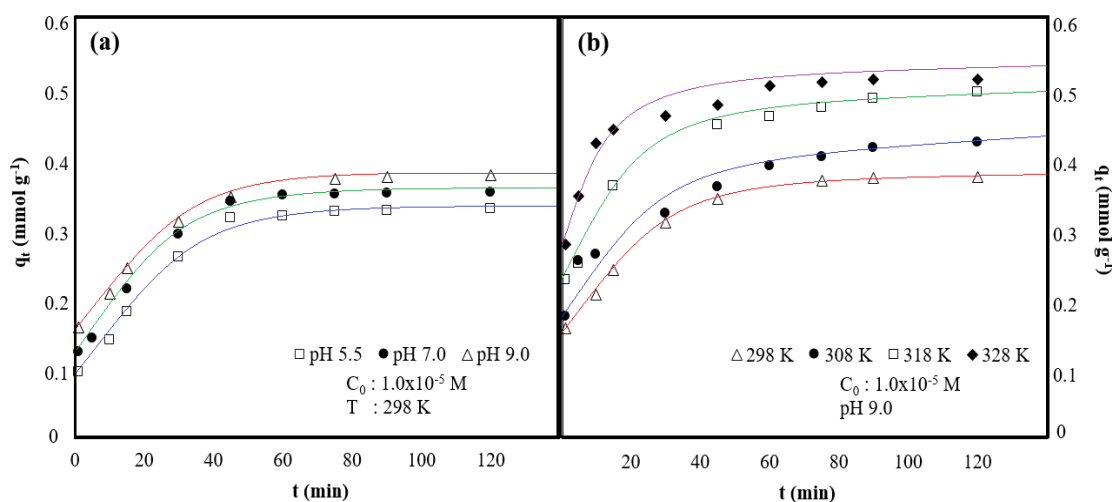


Fig. 1. The effect of (a) solution pH and (b) temperature to the adsorption rate of MB onto TGC

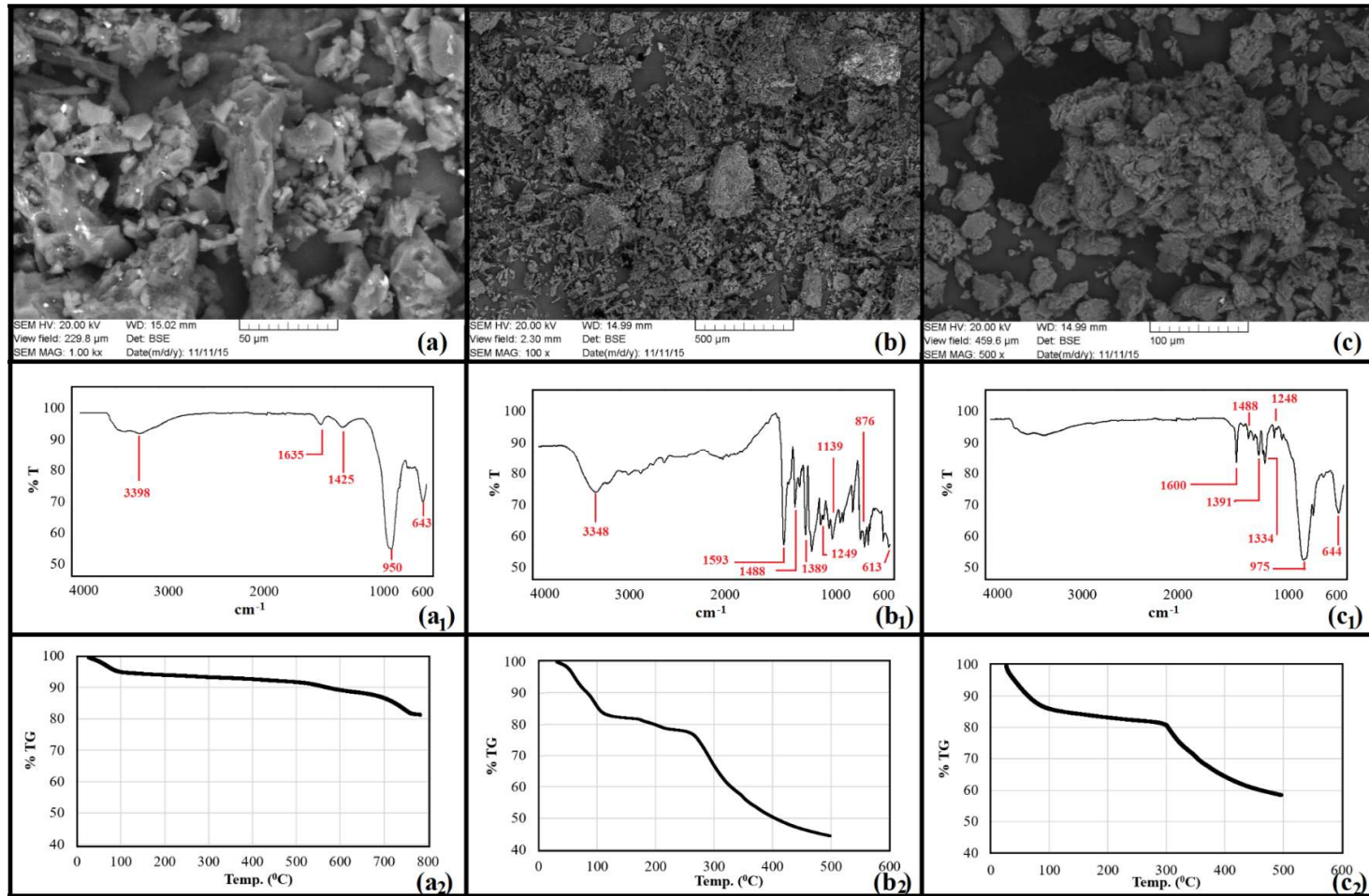


Fig. 2. SEM microphotographs, FTIR spectra and thermal gravimetric analyses of (a, a<sub>1</sub>, a<sub>2</sub>) GC, (b, b<sub>1</sub>, b<sub>2</sub>) MB and (c, c<sub>1</sub>, c<sub>2</sub>) MB adsorbed TGC after 120 m

**Table 1. Parameters of pseudo-first and second order for the adsorption of various parameters of MB onto TGC**

Parameters	Kinetic models								
	Pseudo-first order			Pseudo-second order					
T/K	Initial MB concentration (mol L <sup>-1</sup> ) x 10 <sup>5</sup>	pH	R <sup>2</sup>	q <sub>e</sub> (calculated) (mmol g <sup>-1</sup> )	q <sub>e</sub> (exp.) (mmol g <sup>-1</sup> )	k <sub>2</sub> (gmmol <sup>-1</sup> s <sup>-1</sup> )	R <sup>2</sup>	h (mmol min <sup>-1</sup> g <sup>-1</sup> )	t <sub>1/2</sub> (min)
298	1.0	5.5	0.942	0.342	0.358	0.448	0.988	0.156	6.41
298	1.0	7.0	0.945	0.361	0.376	0.906	0.999	0.335	2.98
298	1.0	9.0	0.968	0.372	0.398	0.364	0.999	0.141	7.09
308	1.0	9.0	0.905	0.425	0.435	0.455	0.998	0.164	6.09
318	1.0	9.0	0.922	0.499	0.506	0.650	0.999	0.195	5.12
328	1.0	9.0	0.932	0.512	0.524	0.785	0.998	0.383	2.61
298	0.5	9.0	0.973	0.181	0.208	0.343	0.989	0.068	14.7
298	2.0	9.0	0.881	0.559	0.612	0.109	0.978	0.066	15.1

As seen in Fig. 2a<sub>2</sub>, b<sub>2</sub> and c<sub>2</sub>, the thermal gravimetric analyzes of TGC, MB and MB adsorbed TGC were measured by thermal gravimetric analyser (TGA). From the TGA curves of a representative sample (Fig. 2a<sub>2</sub>, b<sub>2</sub> and c<sub>2</sub>), we conclude that:

- In the temperature range from 25°C to 105°C, the weight loss due to absorbed water are 6.1% for TGC (Fig. 2a<sub>2</sub>), 15.6% for MB (Fig. 2b<sub>2</sub>) and 14.3% for MB adsorbed TGC (Fig. 2c<sub>2</sub>).
- As shown in Fig. 2a<sub>2</sub>, the second dehydration step observed in the temperature range 105-300°C, corresponds to the release of water molecules, which were in the interlayer space of sample. In the temperature range from 400°C to 700°C, the rapid weight loss (6.5%) is documented by the steep slope of the TGA curve. This is attributed to the dehydroxylation of the sample.
- It can be observed from the profiles of the TGA curves, both MB and MB adsorbed TGC are practically similar. As illustrated in Fig. 2b<sub>2</sub> and c<sub>2</sub> curves, there are two weight loss stages at room temperature -200°C and 200 – 500°C, respectively. For the MB and MB adsorbed TGC, the first stage is attributed to the structural water; the second stage is assigned to the decomposition of MB. Therefore, by comparing TGA scans of MB adsorbed TGC with TGC, the extra weight loss of MB adsorbed TGC should be attributed to the

decomposition of adsorbed MB, and thus the loading ratio of MB can be calculated.

### 3.5 Adsorption Kinetics

In order to examine the controlling mechanism of adsorption process, several kinetic models were used to test the experimental data.

#### 3.5.1 Pseudo-first and second order models

The pseudo first-order equation is generally expressed as follows [30-32]:

$$\ln(q_e - q_t) = \ln q_e - k_1 t \quad (2)$$

If the rate of the adsorption is a second - order mechanism, the pseudo - second -order equation is expressed by Eq. (3) [33]:

$$\frac{t}{q_t} = \frac{t}{q_e} + \frac{1}{k_2 q_e^2} \quad (3)$$

Where  $q_e$  and  $q_t$  (mg g<sup>-1</sup>) are the amount of adsorbed dye at equilibrium and any time  $t$ , respectively, and  $k_1$  is the rate constant of pseudo - first- order adsorption (min<sup>-1</sup>).  $k_2$  is the pseudo-second order rate constant (g mmol<sup>-1</sup> min<sup>-1</sup>). The fitting results are given in Table 1.

The half - adsorption time of the MB,  $t_{1/2}$ , is expressed by Eq. (4):

$$t_{1/2} = \frac{1}{k_2 q_e} \quad (4)$$

**Table 2. Parameters of mass transfer and intra – particle diffusion models for the adsorption of MB onto TGC**

Parameters	Mechanism of adsorption						
	Mass transfer			Intra – particle diffusion			
T/K	Initial MB concentration (mol L <sup>-1</sup> ) x 10 <sup>5</sup>	pH	R <sup>2</sup>	k <sub>int,1</sub> x10 <sup>2</sup> (mmol g <sup>-1</sup> min <sup>-1/2</sup> )	R <sub>1</sub> <sup>2</sup>	k <sub>int,2</sub> x10 <sup>2</sup> (mmol g <sup>-1</sup> min <sup>-1/2</sup> )	R <sub>2</sub> <sup>2</sup>
298	1.0	5.5	0.70	3.70	0.96	0.16	0.99
298	1.0	7.0	0.74	3.96	0.98	0.11	0.94
298	1.0	9.0	0.42	0.34	0.98	0.37	0.88
308	1.0	9.0	0.74	2.91	0.96	1.03	0.94
318	1.0	9.0	0.73	4.79	0.92	1.16	0.97
328	1.0	9.0	0.65	6.00	0.98	0.76	0.68
298	0.5	9.0	0.61	2.55	0.96	0.57	0.92
298	2.0	9.0	0.82	4.56	0.98	0.65	0.59

The initial adsorption rate,  $h$  (min g<sup>-1</sup> min<sup>-1</sup>), is expressed by Eq. (5):

$$h = k_2 q_e^2 \quad (5)$$

The adsorption rate constant  $k_1$  and  $q_e$  were calculated from the plot of  $\ln(q_e - q_t)$  against  $t$  and are not presented in Table 1 because the R<sup>2</sup> values are not very high, and is between 0.88 and 0.97. The values of  $q_e$  and  $k_2$  were estimated from the slope and intercept of plots of  $t/q_t$  vs  $t$  and the corresponding results are also presented in Table 1. The correlation coefficients are much greater in this case, and are in the range of 0.97-0.99, confirming a very good agreement with experimental data. As shown in Table 1, experimental data can be explained by pseudo - second - order kinetic equations.

### 3.5.2 Intra-particle diffusion and mass transfer models

The initial rate of the intraparticle diffusion is calculated by the following Eq. (6) [30]:

$$q_t = k_{int} t_{1/2} + C \quad (6)$$

where  $k_{int}$  is the intraparticle diffusion rate constant (mmol(g min<sup>-1/2</sup>)<sup>-1</sup>) and is given in Table 2. The intraparticle diffusion coefficient for the adsorption of MB was calculated from the slope of the plot of square root of time (min<sup>1/2</sup>) vs. amount of MB adsorbed (mmol g<sup>-1</sup>). Previous studies by various researchers showed that the plot between  $q_t$  and  $t^{1/2}$  represent multi-linearity, which characterizes the two or more steps involved in adsorption process [28,33]. Figures of the plot between  $q_t$  and  $t^{1/2}$  for MB onto TGC

particles not shown but it can be seen that the adsorption process tends to be followed by two phases. It was found that the initial linear portion ended with a smooth curve followed by second linear portion. The two phases in the intraparticle diffusion plot suggest that the adsorption process proceeds by first surface adsorption, and then intraparticle diffusion. The initial curved portion of the plot indicates boundary layer effect while the second linear portion is due to intraparticle or pore diffusion. The calculated intraparticle diffusion coefficient values,  $k_{int,1}$  and  $k_{int,2}$  at different conditions are shown in Table 2. Since  $k_{int,1}$  values for the first part of the plot are high, this step is not a rate - limiting step. The slope of the second linear portion of the plot has been defined as the intraparticle diffusion parameter  $k_{int,2}$  (mmol/(g min<sup>1/2</sup>)) [30,34,35].

For mass transfer, a linear graphical relation between  $\ln [(C_t/C_0)-1(1 + mK)]$  vs.  $t$  was not obtained (equation from [31]). This result indicates that the model mentioned above for the system is not valid. The values of regression coefficient calculated from the equation mentioned above are given in Table 2.

### 3.6 Thermodynamic Parameters

The second – order rate constants are used to estimate the activation energy of the MB adsorption onto TGC using Arrhenius Eq. (7)

$$\ln k_2 = \ln A - \frac{E_a}{R_g T} \quad (7)$$

where;  $E_a$  is the activation energy (Jmol<sup>-1</sup>),  $k_2$  is the rate constant of adsorption (g mmol<sup>-1</sup>s<sup>-1</sup>),  $A$  is the Arrhenius factor, which is the temperature -

independent factor ( $g \text{ mmol}^{-1}\text{s}^{-1}$ ),  $R_g$  is the gas constant ( $8.314 \text{ Jmol}^{-1}\text{K}^{-1}$ ) and  $T$  is the solution temperature (K). The slope of the plot of  $\ln k_2$  vs.  $1/T$  is used to evaluate  $E_a$ , which was found to be  $14.45 \text{ kJmol}^{-1}$ . The magnitude of activation energy gives an idea about the type of adsorption which is mainly physical or chemical. Low activation energies ( $<40 \text{ kJmol}^{-1}$ ) are characteristics for physisorption, while higher activation energies ( $40\text{--}800 \text{ kJmol}^{-1}$ ) suggest chemisorption [34–36]. The result obtained for the adsorption of MB onto TGC indicates that the adsorption process is a physisorption. Therefore, the affinity of MB for TGC may be ascribed to Van der Waals forces and electrostatic attractions between the dye and the surface of the TGC. This low value of  $E_a$  generally indicates diffusion controlled process. We can therefore conclude that the  $E_a$  value calculated from data suggest a diffusion-controlled process, which is a physical step in the adsorption process.

Moreover, the thermodynamic activation parameters of the process such as enthalpy ( $\Delta H^\ddagger$ ), entropy ( $\Delta S^\ddagger$ ) and Gibbs free energy ( $\Delta G^\ddagger$ ) were determined using the Eyring Eq. (8) and Gibbs energy of activation (9) [36].

$$\ln\left(\frac{k_2}{T}\right) = \ln(k_b/h) + \frac{\Delta S^\ddagger}{R_g} - \frac{\Delta H^\ddagger}{R_g T} \quad (8)$$

Moreover, Gibbs energy of activation may be written in terms of entropy and enthalpy of activation:

$$\Delta G^\ddagger = \Delta H^\ddagger - T\Delta S^\ddagger \quad (9)$$

Where  $k_b$  is the Boltzmann constant ( $1.3807 \times 10^{-23} \text{ JK}^{-1}$ ),  $h$  is the Planck constant ( $6.6261 \times 10^{-34} \text{ Js}$ ) and  $R_g$  is the ideal gas constant ( $8.314 \text{ Jmol}^{-1}\text{K}^{-1}$ ). From the plot of  $\ln\left(\frac{k_2}{T}\right)$  against  $1/T$  ( $y = -2290.1x + 0.9628, R^2 = 0.983$ ), the positive value of  $\Delta H^\ddagger$  ( $19.03 \text{ kJmol}^{-1}$ ) confirms the endothermic process, meaning the reaction consume energy. At the same time, the low value of  $\Delta H^\ddagger$  implies that there was loose bonding between the adsorbate molecules and the adsorbent surface [34]. The negative value of the entropy,  $\Delta S^\ddagger$  ( $-22.80 \text{ Jmol}^{-1}\text{K}^{-1}$ ), suggests decreased randomness at the solid/solution interface during the sorption dye ions onto TGC. The values for  $\Delta G^\ddagger$  were found to be positive (about  $+ 26 \text{ kJmol}^{-1}$ ) at all the temperatures indicating the existence of energy barrier for the MB adsorption. Similar results and discussions of

activation parameters such as ( $\Delta H^\ddagger$ ), ( $\Delta S^\ddagger$ ) and Gibbs free energy ( $\Delta G^\ddagger$ ) were given in the literature [37–40].

#### 4. CONCLUSIONS

Some experimental parameters were performed in this study, including the effect of pH, contact time, initial MB concentration and temperatures. In addition, the kinetic and thermodynamic parameters of adsorption of methylene blue onto TGC surface were determined. The experiments were carried out at 120 min contact time. It was determined that the adsorption process was sufficient to reach equilibrium. In order to investigate the mechanism of adsorption, pseudo-first- and second-order kinetic equations, and intraparticle diffusion model have been used to test the experimental data. The rate constants and the related correlation coefficients were determined in order to assess which model provides the best-fit predicted data with experimental results. Pseudo-second-order kinetic equation provided the best-fit to experimental data. The dye uptake process was found to be controlled by intraparticle diffusion. The positive value of the standard Gibbs energy change of the adsorption indicates that the existence of energy barrier for the MB adsorption. The positive value of the standard enthalpy change of the adsorption shows that the adsorption is an endothermic process. Consequently, experimental data obtained from this investigation reveal that physical adsorption is suitable for the attachment of dye into clay as support. TGC has a high potential to adsorb these dye from aqueous solutions. Therefore, it can be effectively used as an adsorbent for the adsorption of this dye.

#### COMPETING INTERESTS

Authors have declared that no competing interests exist.

#### REFERENCES

1. Brookstein DS. Factors associated with textile pattern dermatitis caused by contact allergy to dyes finishes, foam and preservatives. *Dermatol. Clin.* 2009;27: 309–322.
2. Carneiro PA, Umbuzeiro GA, Oliveira DP, Zanoni MVB. Assessment of water contamination caused by a mutagenic textile effluent/dye house effluent bearing



- disperse dyes. J. Hazard. Mat. 2010;174:694–699.
3. Marin MO, Prete VD, Moruno EG, Gonzalez CF, Garc AM, Serrano VG. The development of an activated carbon from cherry stones and its use in the removal of ochratoxin A from red wine. Food Control. 2009;20:298–303.
  4. Bhatnagar A, Jain AK, Mukul MK. Removal of congo red dye from water using carbon slurry waste. Environ Chem. Lett. 2005;2:199–202.
  5. Ramakrishna KR, Viraraghavan T. Dye removal using low cost adsorbents. Water Sci. Technol. 1997;36:189–196.
  6. Javaid M, Saleemi AR, Naveed S, Zafar M, Ramzan N. Anaerobic treatment of desizing effluent in a mesophilic anaerobic packed bed reactor. JPIChE. 2011;39:61–67.
  7. Qian F, Sun X, Liu Y. Removal characteristics of organics in bio-treated textile wastewater reclamation by a stepwise coagulation and intermediate GAC/O3 oxidation process. Chem. Eng. J. 2013;214:112–118.
  8. Kurt E, Koseoglu-Imer DY, Dizge N, Chellam S, Koyuncu I. Pilot-scale evaluation of nanofiltration and reverse osmosis for process reuse of segregated textile dyewash wastewater. Desalination. 2012;302:24–32.
  9. Aziz F, Rehman MSU, Batool A, Muhammad A, Mahmood T. Pretreatment of municipal, industrial and composite wastewater by ozonation. Environ. Process. Eng. 2012;1–2:1–8.
  10. Yasar A, Khalil S, Tabinda AB, Malik A. Comparison of cost and treatment efficiency of solar assisted advance oxidation processes for textile dye bath effluent. Korean J. Chem. Eng. 2013;30: 131–138.
  11. Lotito AM, Fratino U, Bergna G, Iaconi CD. Integrated biological and ozone treatment of printing textile wastewater. Chem. Eng. J. 2012;195–196:261–269.
  12. Asgher M, Bhatti HN. Evaluation of thermodynamics and effect of chemical treatments on sorption potential of citrus waste biomass or removal of anionic dyes from aqueous solutions. Ecol. Eng. 2011;38:79–85.
  13. Jose M, Harsha N, Suhailath K, Mohamed AP, Shukla S. Hydrogen phosphate anions modified hydrogen titanate nanotubes for methylene blue adsorption from aqueous solution: Validating novel method of predicting adsorption capacity. J. Environ. Chem. Eng. 2016;4:1295–1307.
  14. Ali I. New generation adsorbents for water treatment. Chem. Rev. 2012;112:5073–5091.
  15. Ali I, Asim M, Khan TA. Low cost adsorbents for removal of organic pollutants from wastewater. J. Environ. Manag. 2012;113:170–183.
  16. Ali I. The quest for active carbon adsorbent substitutes: Inexpensive adsorbents for toxic metal ions removal from wastewater. Sep. Purif. Rev. 2010;39:95–171.
  17. Auta M, Hameed BH. Preparation of waste tea activated carbon using potassium acetate as an activating agent for adsorption of acid blue 25 dye. Chem. Eng. J. 2011;171:502–509.
  18. Auta M, Hameed BH. Acid modified local clay beads as effective low-cost adsorbent for dynamic adsorption of methylene blue. J. Ind. Eng. Chem. Available:<http://dx.doi.org/10.1016/j.jiec.2012.12.012>
  19. Auta V, Hameed BH. Modified mesoporous clay adsorbent for adsorption isotherm and kinetics of methylene blue. Chem. Eng. J. 2012;198–199:219–227.
  20. Rehman MSU, Munir M, Ashfaq M, Rashid N, Nazar MF, Danish M, Han JI. Adsorption of brilliant green dye from aqueous solution onto red clay. Chem. Eng. J. 2013;228:54–62.
  21. Wang P, Cao M, Wang C, Ao Y, Hou J, Qian J. Kinetics and thermodynamics of adsorption of methylene blue by amagnetic graphene-carbon nanotube composite. Appl. Surf. Sci. 2014;290:116–124.
  22. Hameed BH, Ahmad AA. Batch adsorption of methylene blue from aqueous solution by garlic peel, an agricultural waste biomass. J. Hazard. Mater. 2009;164:870–875.
  23. Lim LBL, Priyantha N, Hei Ing C, Khairud Dahri M, Tennakoon DTB, Zehra T, Suklueng M. *Artocarpus odoratissimus* skin as a potential low-cost biosorbent for the removal of methylene blue and methyl violet 2B. Desalin. Water Treat. 2015;53:964–975.
  24. Dahri MK, Kooh MRR, Lim LBL. Application of *Casuarina equisetifolia* needle for the removal of methylene blue and malachite green dyes from aqueous solution. Alexandria Engineering Journal. 2015;54:1253–1263.

25. Available:<https://www.leaf.tv/articles/green-clay-benefits/> (Accessed 07.12.2016)
26. Williams LB, Haydel SE, Giese Jr RF, Eber DD. Chemical and mineralogical characteristics of French green clays used for healing. *Clays Clay Miner.* 2008;56(4):437–452.
27. Alkan M, Doğan M, Turhan Y, Demirbaş Ö, Turan P. Adsorption kinetics and mechanism of maxilon blue 5G dye on sepiolite from aqueous solutions. *Chem. Eng. J.* 2008;139:213-223.
28. Nandi BK, Goswami A, Purkait MK. Adsorption characteristics of brilliant green dye on kaolin. *J. Hazard. Mat.* 2009;161:387–395.
29. Ghaedi M, Hossainian H, Montazerzohori M, Shokrollahi A, Shojai pour F, Soylak M, Purkait MK. A novel acorn based adsorbent for the removal of brilliant green. *Desalination.* 2011;281:226–233.
30. Weber Jr WJ, Morris JC. Kinetics of adsorption on carbon from solution. *J. Sanit. Eng. Div. ASCE.* 1963;18:31-42.
31. Hunter J. Introduction to modern colloid science. Oxford University Press, New York, USA; 1999.
32. Lagergren S. About the theory of so called adsorption of soluble substances, *Kungl. Sven. Vetenskapskad. Handl.* 1898;24:1–39.
33. Ho YS, McKay G. Sorption of dye from aqueous solution by peat. *Chem. Eng. J.* 1998;70:115–124.
34. Mall ID, Upadhyay SN. Treatment of methyl violet bearing wastewater from paper mill effluent using low cost adsorbents. *J. Indian Pulp. Paper Technol. Assoc.* 1995;7(1):51-57.
35. Kannan N, Sundaram M. Kinetics and mechanism of removal of methylene blue by adsorption on various carbons: A comparative study. *Dyes Pigment.* 2001;51: 25-40.
36. Laidler KJ, Meiser JM. *Physical chemistry.* Houghton Mifflin, New York, NY. 1992;852.
37. Salameh Y, Al-Lagtah N, Ahmad MNM, Allen SJ, Walker GM. Kinetic and thermodynamic investigations on arsenic adsorption onto dolomitic sorbents. *Chem. Eng. J.* 2010;160:440–446.
38. Tayade PB, Adivarekar RV. Adsorption kinetics and thermodynamic study of *Cuminum cyminum* L. dyeing on silk. *J. Environ. Chem. Eng.* 2013;1:1336–1340.
39. Mahmood T, Saddique MT, Naeem A, Mustafa S, Zeb N, Shah KH, Waseem M. Kinetic and thermodynamic study of Cd(II), Co(II) and Zn(II) adsorption from aqueous solution by NiO. *Chem. Eng. J.* 2011;171:935–940.
40. Ferreira BCS, Teodoro FS, Mageste AB, Gil LF, de Freitas RP, Gurgel LVA. Application of a new carboxylate-functionalized sugarcane bagasse for adsorptive removal of crystal violet from aqueous solution: Kinetic, equilibrium and thermodynamic studies. *Industrial Crops and Products.* 2015;65:521–534.

© 2016 Demirbaş and Nas; This is an Open Access article distributed under the terms of the Creative Commons Attribution License (<http://creativecommons.org/licenses/by/4.0>), which permits unrestricted use, distribution, and reproduction in any medium, provided the original work is properly cited.

*Peer-review history:*  
The peer review history for this paper can be accessed here:  
<http://sciencedomain.org/review-history/17313>